Quantification of myoglobin deoxygenation and intracellular partial pressure of O2 during muscle contraction during haemoglobin-free medium perfusion

Quantification of Myoglobin Deoxygenation and Intracellular PO_2 during Muscle Contraction under Hb-free Medium Perfusion

Hisashi Takakura[1], Kazumi Masuda[2], Takeshi Hashimoto[3], Satoshi Iwase[4], Thomas Jue[5]

[1]The Graduate School of Natural Science and Technology, and [2]Faculty of Human Sciences, Kanazawa University, Kanazawa 920-1192, Japan, [3]The Graduate School of Life Science, University of Hyogo, Kamigori 678-1297, Japan, [4]Department of Physiology, Aichi Medical University, Nagakute 480-1195, Japan, [5]Department of Biochemistry and Molecular Medicine, University of California Davis, Davis 95616-8635, USA

Running Title: Change in intracellular PO_2 at onset of contraction

Key Words: intracellular PO_2, NIRS, hindlimb perfusion, respiration, skeletal muscle

Table of Content: Page No

Correspondence:
Kazumi MASUDA, Ph. D., Professor
Faculty of Human Sciences, Kanazawa University,
Kakuma-machi, Kanazawa-city, Ishikawa, 920-1192, Japan.
E-mail: masuda@ed.kanazawa-u.ac.jp
Phone: [+81] 76-264-5568, Fax: [+81] 76-234-4100

Abstract

Although the O_2 gradient regulates O_2 flux from the capillary into the myocyte to meet the energy demands of contracting muscle, intracellular O_2 dynamics during muscle contraction remain unclear. Our hindlimb perfusion model allows the determination of intracellular myoglobin (Mb) saturation ($S_{mb}O_2$) and intracellular oxygen tension of myoglobin ($P_{mb}O_2$) in contracting muscle using near infrared spectroscopy (NIRS). The hindlimb of male Wistar rats was perfused from the abdominal aorta with a well-oxygenated hemoglobin (Hb)-free Krebs-Henseleit buffer. The deoxygenated Mb (Δ[deoxy-Mb]) signal was monitored by NIRS. Based on the value of Δ[deoxy-Mb], $S_{mb}O_2$ and $P_{mb}O_2$ were calculated and the time course was evaluated by an exponential function model. Both $S_{mb}O_2$ and $P_{mb}O_2$ started to decrease immediately after the onset of contraction. The steady state values of $S_{mb}O_2$ and $P_{mb}O_2$ progressively decreased with relative work intensity or muscle oxygen consumption. At the maximal twitch rate, $S_{mb}O_2$ and $P_{mb}O_2$ were 49% and 2.4 mmHg, respectively. Moreover, the Mb O_2 release rate at the onset of contraction increased with muscle oxygen consumption. These results suggest that at the onset of muscle contraction, Mb supplies O_2 during the steep decline in $P_{mb}O_2$, which expands the O_2 gradient to increase the O_2 flux to meet the increased energy demands.

Abbreviations

CO, carbon monoxide; DO_2, O_2 diffusion conductance; ^{1}H-MRS, ^{1}H-magnetic resonance spectroscopy; Hb, hemoglobin; Mb, myoglobin; $\dot{m}VO_2$, muscle oxygen consumption; $\Delta\dot{m}VO_2$, the change in $\dot{m}VO_2$ from the resting value; NIRS, near infrared spectroscopy; PO_2, oxygen tension; $P_{mb}O_2$, intracellular oxygen tension; $P_{cap}O_2$, microvascular oxygen tension; $S_{mb}O_2$, oxygen saturation of myoglobin; Δ[deoxy-Mb], changes in the NIRS signal associated with the concentration of deoxygenated Mb; Δ[oxy-Mb], changes in the NIRS signal associated with the concentration of oxygenated Mb; BL, the baseline value; AP, the amplitude between BL and the steady-state value component; $_{0.63}$AP/MRT, the mean rate of change to 63% of the AP value; TD, the time delay between the start of contraction and the appearance of the $P_{mb}O_2$ and $S_{mb}O_2$ signal; τ, the exponential time constant of the kinetics of the $P_{mb}O_2$ and $S_{mb}O_2$; MRT, the mean response time of the kinetics that equals TD + τ.

Introduction

Cellular respiration is influenced by a wide range of mechanisms including the response of the cardiovascular and metabolic systems to meet the changing energy demands in muscle. Although the O_2 gradient between the microvasculature and myocyte is particularly important for O_2 diffusion to sustain cellular respiration in contracting muscle, intracellular O_2 dynamics during muscle contraction remain unknown.

A phosphorescence quenching technique has sometimes been used to determine microvascular oxygen tension ($P_{cap}O_2$) in contracting muscle (Behnke *et al.* 2001; McDonough *et al.* 2005). In healthy rodent skeletal muscle, the $P_{cap}O_2$ decreased exponentially at the onset of 1 Hz contractions with an approximate 20 sec time delay (Behnke *et al.* 2001). In contrast, the estimated muscle oxygen consumption ($m\dot{V}O_2$) calculated from capillary red blood cell flux and $P_{cap}O_2$ increased immediately after onset of the muscle contraction. A change in $m\dot{V}O_2$ without a corresponding change in $P_{cap}O_2$ would imply an increased O_2 diffusing capacity (DO_2), according to Fick's law. However, the study did not measure a key parameter, the kinetics of $P_{mb}O_2$ (Behnke *et al.* 2002; Poole *et al.* 2007). Without a $P_{mb}O_2$ dynamics measurement, defining the limiting factor as DO_2 at the onset of exercise remains debatable.

The $P_{mb}O_2$ during exercise can play a key role in regulating the $\dot{V}O_2$ in exercising muscle (Molé *et al.* 1999). In order for O_2 delivery from capillaries to mitochondria to increase to accommodate the increasing oxygen demand, $P_{mb}O_2$ should fall so as to increase the O_2 gradient from the capillary to the muscle cell during exercise. In fact, ^{1}H-magnetic resonance spectroscopy (^{1}H-MRS) experiments have shown an increasing signal intensity of deoxy-Mb His F8 $N_\delta H$ during contraction in human leg muscle, suggesting a fall in intracellular PO_2 (Molé *et al.* 1999; Richardson *et al.* 1995). However, while Richardson *et al.*

(1995) have reported that Mb does not desaturate in proportion to increased work output, Molé *et al.* (1999) have shown that Mb becomes increasingly desaturated with increasing oxygen consumption or power output during progressive plantar flexion exercise. Moreover, Molé *et al.* (1999) indicate that $P_{mb}O_2$ can modulate the O_2 gradient. The discrepancy between the two studies may originate from differences in the muscle group studied, the subject population, and/or the MRS acquisition/processing methodology.

Near infrared spectroscopy (NIRS) can investigate the dynamics of tissue oxygenation in contracting muscle during the transition from rest to work with high time resolution, if it can discriminate the Mb from the Hb interference. Indeed, NIRS measurement allows detection of the Mb desaturation kinetics under Hb-free buffer perfused conditions, indicating a significant contribution of signals derived from Mb to the NIRS signal and progressive desaturation of Mb with work intensity (Masuda *et al.* 2010).

The present study utilizes NIRS to investigate Mb desaturation and $P_{mb}O_2$ kinetics during muscle contraction at different work and intensity or $m\dot{V}O_2$ levels. Mb desaturates immediately at the onset of contraction, which reflects a steep decline in the $P_{mb}O_2$ and a sudden widening of the O_2 gradient changes to meet the increased metabolic demand. Moreover, $P_{mb}O_2$ progressively decreases as contraction force and $m\dot{V}O_2$ increase.

Materials and Methods

Experimental Animals and Preparation of Hindlimb Perfusion

All experimental procedures performed in the present study conformed to the Fundamental Guidelines for Proper Conduct of Animal Experiment and Related Activities in Academic Research Institutions (Published by the Ministry of Education, Culture, Sports,

Science and Technology. Japan) and was approved by the ethics committee for Animal Experimentation of Kanazawa University (Protocol#: AP-080943).

Male Wistar rats (9 weeks old, 257-295 g body weight, n = 6) were used for the experiments in this study. All rats were housed in a temperature-controlled room at 23 ± 2 °C with a light-dark cycle of 12 h and maintained on a commercial diet with water ad libitum.

All surgical procedures were performed under pentobarbital sodium anesthesia (45 mg/kg intraperitoneal). Physiological body temperature was maintained using a heated mat. Preparation of isolated rat hindlimb and the perfusion apparatus were described in a previous report (Masuda *et al.* 2010). In brief, the abdominal wall was first incised from the pubic symphysis to the xiphoid process. The spermary, testis, and inferior mesenteric arteries and veins were ligated, and the spermaries, the testes, and part of the descending colon were excised, together with contiguous adipose tissue. The caudal artery and internal iliac artery and vein were also ligated. Ligatures were placed around the neck of the bladder, the anterior prostate and the prostate gland. The vessels that supply the subcutaneous region were also ligated. Following these ligations, the inferior epigastric, iliolumbar and renal arteries and veins were ligated as well as the coeliac axis and portal vein. A further ligature was placed around the tail. After the euthanasia by injection of 1M KCl solution into the heart, an Hb-free Krebs-Henseleit buffer (NaCl, 118 mM; KCl, 5.9 mM; KH_2PO_4, 1.2 mM; $MgSO_4$, 1.2 mM; $CaCl_2$, 1.8 mM; $NaHCO_3$, 20mM; Glucose, 15 mM) was perfused into the abdominal aorta in a flow-through mode at a constant flow.

The flow rate was set to 22 ml/min corresponding to a perfusion pressure of around 90 mmHg, based on the methods reported by Shiota and Sugano (1986). In the present study, average perfusion pressure was 88.7 ± 3.7 mmHg when the flow rate was set at 22 ml/min. Therefore, the perfusion resistance (ml/min/mmHg) was also unchanged throughout the perfusion period (4.0 ± 0.1 ml/min/mmHg). Besides, no symptom of edema in the hindlimb

was confirmed at the given flow rate. After cannulating into the abdominal aorta, the contralateral (right hindlimb) common iliac artery was ligated. The Krebs-Henseleit buffer containing Heparin (1000 U/l) was perfused into the hindlimb for 10 min from the beginning of the perfusion to prevent clotting of the blood and to wash out blood from the hindlimb.

The perfusate and the muscle temperature were maintained at 37 °C. The rat hindlimb was perfused with buffer equilibrated with 95%O_2 + 5%CO_2 for 30 min before and throughout the exercise protocol. The presence of CO_2 maintained the pH between 7.3-7.4. The effluent was collected from the inferior vena cava in order to measure the $m\dot{V}O_2$ and the concentration of lactate and pyruvate.

Twitch Contraction Protocol

The buffer was equilibrated for 30 min from the beginning of the perfusion experiments. The sciatic nerve of the left hindlimb was then exposed and connected to two parallel stainless steel wire electrodes (Unique Medical, Tokyo, Japan) and the Achilles' tendon was connected to a sensitive strain gauge with a string (MLT500/D, AD Instrument, Castle Hill, NSW, Australia). Slack in the string was removed by several brief tetanic contractions. To elicit a series of isometric twitch contractions, electric stimuli were delivered to the muscle at its optimum length, at which the muscle generated peak tension, via stainless electrodes on the sciatic nerve. The stimulation consisted of a single square wave (delay: 10 μsec, duration: 1 msec) controlled by an electro stimulator system (Model RU-72, Nihon Koden, Tokyo, Japan). The stimulation was 1 Hz of frequency for 120 sec (120 twitch contractions). The target tension was controlled by changing the voltage of the stimuli to obtain 50~100% of peak tension under buffer-perfused conditions (3-8 volts). The twitch tension was calculated as the average of a series of contractions. Increasing the stimulation voltage in order to increase the force of contraction recruits nerve fibers that are closest to the

stimulating electrodes, and in reverse order with large neurons supplying fast, glycolytic muscle fibers being preferentially recruited first.

Intracellular Oxygenation

An NIRS instrument (NIRO-300 + Detection Fiber Adapter Kit, Hamamatsu Photonics, Shizuoka, Japan) was used to measure the oxygenation of Mb. The distance between the photodiode and the LED was fixed at 10 mm. The toe of the foot was secured by a clamp with the rat laid on its back. After that, the NIRS probes were firmly attached to the skin of the gastrocnemius muscle and were fixed by clamps on both sides of the muscle. During the initial period, for at least 30 sec before the start of contraction, the average fluctuation in the NIRS signals was adjusted to a reference value of zero. After the exercise protocol, the anoxic buffer, equilibrated with 95%N_2 + 5%CO_2 gas was perfused for 30 min to obtain the maximal Mb desaturation value. The equilibrium period with the anoxic buffer was initiated after a 5 min recovery and after the NIRS signals had returned to baseline level. After 30 min, the NIRS signal reached a steady state. The muscle then received electrical stimulation to contract for 2 min. No further increase in Δ[deoxy-Mb] signal was evident. The final Δ[deoxy-Mb] signal intensity served as the normalization constant for 100% Mb deoxygenation.

Data acquisition

The sampling rate for the NIRS data was 1 Hz. The other parameters (tension, perfusion pressure, O_2 content at the inflow and outflow) were collected using a data acquisition system (PowerLab 8SP, AD Instruments, Australia) at a sampling rate of 1 kHz. All the data were transferred to a personal computer with acquisition software (Chart ver. 5.5.6. AD Instruments)

Data Analysis

A simple moving average smoothed the Δ[deoxy-Mb] and the Δ[oxy-Mb] NIRS signal using a rolling average of 5 points, which correspond to a time frame of 5 sec (Box *et al.* 1978). The Δ[deoxy-Mb] kinetics were calibrated against two different values of the NIRS signal: one at rest and the other during steady state with anoxia buffer perfusion. These values correspond to the initial Mb desaturation of 10% and the final Mb desaturation of 100%, respectively. While the $S_{mb}O_2$ at rest could not be determined by NIRS, the value was assumed to be 90% based on the previous studies that reported the $S_{mb}O_2$ at rest was greater than 90% (Chung *et al.* 2005; Richardson *et al.* 2006).

The %Δ[deoxy-Mb] plots were converted to $S_{mb}O_2$ plots using the following equation;

$$S_{mb}O_2\ (\%) = 100 - \%\Delta[\text{deoxy-Mb}]$$

The $S_{mb}O_2$ kinetics shows no evidence for any slow component of Mb desaturation. Therefore, the $S_{mb}O_2$ plots were fitted by the following single exponential equation to calculate the kinetics parameters using an iterative least-squares technique by means of a commercial graphing/analysis package (KaleidaGraph 3.6.1).

$$S_{mb}O_2\ (\%) = BL + AP\ [1 - \exp^{-(t - TD)/\tau}]$$

The parameter values, where BL was the baseline value, AP was the amplitude between BL and the steady-state value during the exponential component, TD was the time delay between the start of contraction and the appearance of the $S_{mb}O_2$ signals, and τ was the time constant of the kinetics of the $S_{mb}O_2$ signal. The $S_{mb}O_2$ kinetics were modeled as an

exponential function. Since $\dot{m}VO_2$ increases rapidly without any time delay, the mean response time (MRT) calculated by TD + τ was used as an effective parameter of the response time for Mb deoxygenation at the onset of muscle contraction (Behnke *et al.* 2002; Rossiter *et al.* 1999). Moreover, MRT indicates the time to require to reach 63% of AP. Dividing 63% of AP by MRT gives a value for the time-dependent change in Mb deoxygenation. The parameter $_{0.63}$AP/MRT for $S_{mb}O_2$ shows the Mb O_2 release rate, which indicates the amount of oxygen released by Mb per unit time at the onset of exercise. The Mb O_2 release rate was calculated by using the following equation:

$$\text{Mb } O_2 \text{ release rate} = (_{0.63}\text{AP} / \text{MRT})\ [\text{Mb}]$$

where the $_{0.63}$AP/MRT for $S_{mb}O_2$ was Mb deoxygenation rate in %/sec, and [Mb] in the hindquarter was 0.119 ± 0.023 μmol/g tissue. Inserting this value for Mb into the equation led to the determination of the Mb O_2 release rate in μmol/g/min.

Based on the result of the $S_{mb}O_2$ kinetics parameters, the model $S_{mb}O_2$ kinetics was re-constructed. The model $S_{mb}O_2$ kinetics was converted to $P_{mb}O_2$ using the following equation;

$$P_{mb}O_2\ (\text{mmHg}) = (S_{mb}O_2 / (1 - S_{mb}O_2))\ P_{50}$$

where P_{50} is the partial oxygen pressure required to half-saturate Mb and a P_{50} of 2.4 mmHg was used for the equation, assuming a muscle temperature of 37 ˚C (Schenkman *et al.* 1997). The calculated $P_{mb}O_2$ plots were mathematically evaluated to get the MRT of its kinetics by using the same single exponential equation as for $S_{mb}O_2$. The $_{0.63}$AP/MRT for $P_{mb}O_2$ indicates decremental rate of $P_{mb}O_2$ at the onset of muscle contraction. The $P_{mb}O_2$ at the steady state

was calculated by directly using the value for $S_{mb}O_2$ at the steady state. Moreover, since the partial pressure of O_2 corresponds to a specific amount of dissolved O_2 in solution, intracellular [O_2] was calculated from $P_{mb}O_2$ value at rest and at each exercise intensity using the following equation.

$$\text{Intracellular } [O_2] \text{ } (\mu M) = P_{mb}O_2 \text{ x } O_2 \text{ solubility}$$

where $P_{mb}O_2$ is in mmHg, and the solubility of O_2 in buffer is 0.00135 μmol/ml/mmHg at 37 ˚C (Philip and Dorothy, 1971).

Muscle oxygen consumption

$\dot{m}VO_2$ was calculated from the arteriovenous oxygen content difference multiplied by the flow rate, using the equation:

$$\dot{m}VO_2 \text{ (μmol/g/min)} = \text{flow rate x } ((PO_2\text{in} - PO_2\text{out}) \text{ x } O_2 \text{ solubility}) / \text{muscle weight}$$

where flow rate is the flow in ml/min, and PO_2in and PO_2out are the arterial and venous oxygen tensions after adjusting for the vapor pressure of water. Inflow PO_2 and outflow PO_2 were measured continuously using two O_2 electrodes (5300A, YSI, USA) along tubing before and after perfusing to the hindlimb. The vapor pressure at 37 ˚C is 47.03 mmHg. The solubility of oxygen in the buffer is 0.00135 μmol per ml per mmHg at 37 ˚C (Philip and Dorothy 1971). The $\dot{m}VO_2$ at rest and during muscle contraction was calculated by using the values of PO_2in – PO_2out averaged over 15 sec at the steady state condition before and during muscle contraction. Also, the average rate increase in $\dot{m}VO_2$ was calculated by dividing $\dot{m}VO_2$ by 2 min, the period of muscle contraction, because the response time of the O_2

electrodes was too slow to follow the on-kinetics of $m\dot{V}O_2$.

Tissue Preparation and Optical Measurement

After the buffer perfusion, the hindlimb muscles were isolated and immediately weighed, thoroughly minced using stainless steel scissors, and homogenized in an ice bath with phosphate buffer (0.04 M, pH 6.6) bubbled with carbon monoxide (CO). The homogenate was then separated by centrifugation at 12,000 *g* for 30 min at 4 ˚C. The clear supernatant was decanted into a small glass tube and again equilibrated with CO to ensure binding to Mb. The optical density at 538 nm (ß band) and 568 nm (α band) was used for calculation of both the Hb and Mb concentration in the muscle tissue as described in a modified Reynafarje method (Masuda *et al.* 2008).

Statistical Analyses

All data are expressed as the mean ± SD. Differences between tension levels were examined using repeated measures ANOVA. The Tukey-Kramer's post-hoc test was applied if ANOVA indicated a significant difference. Pearson's correlation coefficient was calculated when the relationship between two variables was evaluated. The level of significance was set at $p < 0.05$.

Results

Figure 1 shows a wave pattern of a single contraction and the time-course change of the twitch tension at each exercise intensity. An isometric twitch contraction was evoked by stimulating the sciatic nerve electrically. The stimulation consisted of a single square wave

(delay: 10 μsec, duration: 1 msec) controlled by an electro stimulator system. Twitch contractions typically show a staircase effect. Twitch contraction showed staircase effect of 17.2 ± 4.2%, 21.8 ± 5.7%, and 20.9 ± 12.0% at 50, 75 and 100% of maximal contraction, which lasted for a total of 120 sec. However, these staircase effects do not affect the Mb desaturation rate, which shows no evidence of a slow component. The muscle also shows no sign of fatigue, even during the highest stimulation intensity.

Table 1 summarizes twitch tensions, $m\dot{V}O_2$, rate increase in $m\dot{V}O_2$ and O_2 release rate of Mb during contractions at different intensities. As the muscle tension increased significantly from 382 mN to 738 mN, the $m\dot{V}O_2$ also increased from 0.46 μmol/g/min at rest to 0.56-0.69 μmol/g/min during muscle contraction. Moreover, rate increase in $m\dot{V}O_2$ and Mb O_2 release rate significantly increase with the tension level. The lactate to pyruvate ratio (L/P) remains constant and shows no significant increase from the resting muscle value (Bylund-Fellenius *et al.* 1981). If oxygen availability were limiting, lactate level should rise, as anaerobic glycolysis starts. Indeed, the L/P increases during perfusion with anoxia buffer ($95\%N_2$) increases. O_2 availability and delivery can sustain maximal contraction with no sign of fatigue.

Figure 2 shows representative Δ[deoxy-Mb] and Δ[oxy-Mb] kinetics during different levels of twitch contractions and under anoxic-perfusion as assessed by NIRS. The Roman numerals I, II and III represent the NIRS signal response to 1 Hz twitch contractions at 50%, 75% and 100% of maximal twitch tension. In protocol IV, the non-contracting muscle received a perfusated $95\%N_2 + 5\%CO_2$.

The Δ[deoxy-Mb] and Δ[oxy-Mb] signals increased and decreased at the onset of contraction, respectively. The AP of Δ[deoxy-Mb] kinetics increases to 4-15 μmol•cm as muscle tension rises (states I-III). The Δ[deoxy-Mb] and Δ[oxy-Mb] signal under perfusion with $95\%N_2 + 5\%CO_2$ rose and declined further than the signal observed during protocols

I-III. The NIRS signals reached a steady state within 10 min. The steady state value of Δ[deoxy-Mb] obtained under anoxic-perfusion was assumed to represent fully desaturated Mb ($S_{mb}O_2$ = 0%). Mb saturation during the resting condition was assumed to be 90% saturated.

Figure 3 shows the kinetics of $S_{mb}O_2$ and $P_{mb}O_2$ during maximal twitch contraction. The plot fits the representative data from a single experiment using protocol III. The Δ[deoxy-Mb] was used to calculate the $S_{mb}O_2$, which (A) declines with an MRT of 45 sec. The corresponding $P_{mb}O_2$ curve (B), converted from $S_{mb}O_2$, shows a faster, steeper decline than the $S_{mb}O_2$ curve and exhibits a shorter MRT of 28 sec. At the maximal twitch tension, $S_{mb}O_2$ and $P_{mb}O_2$ reached the respective values of 49% and 2.4 mmHg .

Table 3 summarizes the kinetic parameters for $S_{mb}O_2$ and $P_{mb}O_2$ during different intensities of twitch contraction. The $S_{mb}O_2$ and $P_{mb}O_2$ during exercise decreased, and the MRT for $S_{mb}O_2$ and $P_{mb}O_2$ kinetics also decreased as work intensity rose ($p < 0.05$).

Figure 4 shows the relationship between $S_{mb}O_2$ and relative work intensity. The work intensity was normalized by maximal twitch tension in each animal. $S_{mb}O_2$ decreased significantly as work intensity increased. The steady state level of $S_{mb}O_2$ declined from 90% at rest to 70.7 ± 7.1%, 59.2 ± 7.4% and 49.3 ± 7.3% at 50%, 75% and 100% of maximal contraction, respectively.

Figure 5 shows the relationship between intracellular [O_2] and $\Delta m\dot{V}O_2$ during twitch contraction. The intracellular [O_2] was based on the Mb equilibrium with $P_{mb}O_2$. The intracellular [O_2] decreased sharply from 29.2 μM at rest to 8.5 ± 3.4 μM, 5.0 ± 1.8 μM and 3.3 ± 1.0 μM at each increased work level, while the value of intracellular [O_2] decreased exponentially with $\Delta m\dot{V}O_2$.

Figure 6 shows the relationship between Mb O_2 release rate at the onset of contraction and $\Delta m\dot{V}O_2$. The Mb O_2 release rate (1.4 ± 0.5, 2.8 ± 0.5, and 4.2 ± 0.7 10^{-2} μmol/g/min) increased progressively with contraction force and $\Delta m\dot{V}O_2$.

Discussion

Intracellular $S_{mb}O_2$ and $P_{mb}O_2$ during muscle contraction

At the onset of muscle contraction, Mb desaturates immediately and rapidly in an exponential manner and reaches a steady state level, which depends upon the work intensity. As the work intensity and $m\dot{V}O_2$ increase, the steady-state level of $S_{mb}O_2$ falls from 90% at rest to 71%, 59%, and 49% at 50%, 75%, and 100% of maximal contraction. The progressive Mb desaturation with increased work agrees with the ^{1}H-MRS observation in contracting human leg muscle (Molé *et al.* 1999). $P_{mb}O_2$ during contraction decreases correspondingly from 6.3 to 2.4 mmHg.

Even as O_2 tension falls during muscle contraction, it never reaches a critical $P_{mb}O_2$ to limit respiration or oxidative phosphorylation (Kreutzer *et al.* 1992) or $m\dot{V}O_2$ (Table 1). Under all contraction conditions, the L/P remains constant and shows no presence of hypoxemia or ischemia.

In fact, as PO_2 falls with work intensity, $m\dot{V}O_2$ rises. From an enzyme kinetics vantage, the rising $m\dot{V}O_2$ with increased contraction intensity in the face of a declining PO_2 raises questions about O_2 as the limiting substrate in regulating the cytochrome reaction rate. If the O_2 supply alone regulates the respiration, then the rising $m\dot{V}O_2$ requires an increased O_2 supply instead of the observed decrease (Chung *et al*. 2005; Jue 2004).

O_2 Gradient

As muscle contraction begins, the $P_{mb}O_2$ decreases immediately to expand the O_2 gradient ($\Delta PO_2/\mu m$) from the capillary to the cell in order to meet the increased energy demand, as expressed in the following equation:

$$\dot{m}VO_2 = k\, DO_2\, (P_{cap}O_2 - P_{mb}O_2)$$

where DO_2 is the O_2 diffusion conductance and $P_{cap}O_2$ is the PO_2 in the capillary. In the constant-flow hindlimb model, DO_2 does not contribute significantly, since a 30-min equilibrium period elicited a flow-induced vasodilatation. The perfusive O_2 conductance remains constant (Hepple *et al.* 2003).

As $\dot{m}VO_2$ rises with muscle contraction, $P_{cap}O_2$ and/or $P_{mb}O_2$ must then change to enhance the O_2 flux into the cell. However, studies have shown that $P_{cap}O_2$ actually decreases from 31.4 (at rest) to 21.0 mmHg during 1 Hz maximal twitch contractions (Δ10.4 mmHg, Behnke *et al.* 2001). If the O_2 gradient has any significant role, then the $\Delta P_{mb}O_2$ must decline even further. Indeed, the $\Delta P_{mb}O_2$ exceeds the $\Delta P_{cap}O_2$ (Δ19.2 mmHg vs. Δ10.4 mmHg). The increase in $\dot{m}VO_2$ during muscle contraction depends then on the expansion of O_2 gradient as shown in Table 4.

Such an expansion of the O_2 gradient does not appear localized only to the buffer perfused hindlimb model, because buffer carries less O_2 than blood. In contracting human skeletal muscle, all ^{1}H-MRS data show Mb desaturation, consistent with a decreased intracellular $P_{mb}O_2$ (Molé *et al.* 1999; Richardson *et al.* 1995). Furthermore, Molé et al. (1999) has indicated that the $P_{mb}O_2$ drops progressively and reaches 3.1 mmHg at peak gastrocnemius muscle contraction.

Change in the Kinetics of $S_{mb}O_2$ and Mb O_2 release rate with Oxygen Demand

The $P_{cap}O_2$, however, does not start to change until about 20 sec, after the onset of muscle contraction. Yet $\dot{m}VO_2$ has already increased. Some researchers have postulated that during this initial period, capillary to cell distance must adjust to increase the DO_2, which increases the O_2 flux to match the rising $\dot{m}VO_2$ (Behnke *et al.* 2001). These researchers have

assumed the O_2 gradient does not play a significant role. However, the present study shows a rapid drop in intracellular $P_{mb}O_2$ and indicates that the O_2 gradient widens quickly.

Even as the O_2 gradient widens and $\dot{m}VO_2$ rises immediately, vascular O_2 flux still does not provide a significant amount of the initial O_2, since $P_{cap}O_2$ appears constant for about 20 sec. Instead, the initial O_2 comes in part from Mb, as evidenced by the rapid fall in $S_{mb}O_2$. Mb releases its O_2 at rate of 1.4 ± 0.5 to 2.8 ± 0.5 and 4.2 ± 0.7 10^{-2}μmol/g/min as the work intensity increases. Even though Mb supplies the primary source of O_2 at the onset of contraction, it provides only about 30% of the average rate of increase in $\dot{m}VO_2$ from 5.3 ± 1.8 to 7.8 ± 1.5 to 10.9 ± 3.4 10^{-2}μmol/g/min^2. However, because of insufficient response time of the O_2 electrodes to allow analysis of $\dot{m}VO_2$ on-kinetics, the limited time resolution of the $\dot{m}VO_2$ precludes currently an accurate assessment of the O_2 contribution of Mb at the onset of contraction. It may provide all the O_2 at the start of contraction. Such a view implies at least a biphasic increase in $\dot{m}VO_2$, consistent with previous reports (Molé *et al.* 1999; Whipp *et al.* 1999).

Contracting human leg muscle also shows Mb desaturates with a time constant of about 25 sec. Indeed, investigators have interpreted the Mb desaturation kinetics as an index of intracellular $\dot{m}VO_2$ and have suggested a mechanism underlying the biphasic increase in $\dot{m}VO_2$ as muscle contraction commences (Chung *et al.* 2005).

Mb as an O_2 buffer

MRT of $P_{mb}O_2$ provides insight into role of Mb as an immediate O_2 source. The investigation using isolated myoglobin-free myocytes from *Xenopus laevis* showed 35.2 ± 5.1 sec in MRT for ~20 mmHg of net depression in intracellular PO_2 during tetanic contractions (Kindig *et al.* 2003). The present study observes an MRT of 27.7 ± 3.1 sec. The slower MRT in *Xenopus laevis* myocyte may arise from the lack of Mb facilitated O_2 transport, and

therefore contracting myocytes require a significantly greater extracellular PO_2 to achieve a given $\dot{m}VO_2$ (Hogan *et al.* 2001; Kindig *et al.* 2003). The present study suggests that Mb provides an immediate O_2 source for the sudden rise in mitochondrial respiration.

Both the perfused hindlimb and human leg experiments point to a similar conclusion: at the start of contraction, a sudden mismatch of O_2 supply and demand appears. Mb buffers the sudden increase in O_2 demand as respiration rises rapidly (Molé *et al.* 1999; Chung *et al.* 2005).

The relationship between $P_{mb}O_2$ kinetics and muscle oxygen consumption

At the highest muscle contraction intensity employed in the present study $P_{mb}O_2$ began to decrease with an MRT of 25 sec while the MRT of $P_{cap}O_2$ was 40.9 sec at 1 Hz muscle contraction (Behnke *et al.* 2001). Therefore, the MRT of $P_{mb}O_2$ is shorter than that for $P_{cap}O_2$ at maximal muscle contraction. This difference suggests that the presence of Mb allows the intracellular O_2 environment to adjust more effectively to the abrupt increase in oxygen demand at the onset of muscle contraction, before the microcirculatory O_2 environment adapts. Mitochondrial respiration accelerates without a discernible delay after the onset of the muscle contraction (Balaban *et al.* 2003). In fact, $\dot{m}VO_2$ begins to increase without a time delay during muscle contraction (Behnke *et al.* 2002). The 23 sec MRT of $\dot{m}VO_2$ is consistent with the 25 sec MRT for $P_{mb}O_2$ observed in human leg studies (Behnke *et al.* 2002; Chung *et al.* 2005).

Limitations of the NIRS perfusion model for the determination of PO_2

Some studies have pointed out the importance of surprisingly large extracellular PO_2 gradients (Gnaiger *et al.* 1995). However, intracellular PO_2 gradients may also increase at increased O_2 flux, so that they affect mitochondrial respiration as a consequence of decreased

cytoplasmic O_2 concentration surrounding mitochondria in the "anoxic core" (Takahashi *et al.* 1998, 1999). Taken together, significant gradients of Mb oxygenation could be produced in the cytoplasm of the *in vivo* heart (Takahashi *et al.* 2000). On the other hand, in the classical view, Mb facilitates O_2 transport within exercising myocytes (Wittenberg and Wittenberg 1989) and that produces relatively homogeneous cytoplasmic PO_2 distribution even during maximal aerobic work (Honig *et al.* 1997; Jones 1986). Mb translational diffusion in the cell, however, appears too slow to have a significant transport role in the steady state (Papadopoulos *et al.* 2001; Lin *et al.* 2007b). However, it may still play a significant role in the transient state, when the PO_2 falls precipitously (Lin *et al.* 2007a). Unfortunately, the NIRS measurements cannot shed insight into these issues. The $P_{mb}O_2$ gradient and Mb facilitated O_2 diffusion within the cell remain controversial.

The previous ^{1}H-MRS study did not detect the proximal histidyl $N_\delta H$ F8 of deoxy-Mb under resting conditions, even though this experimental technique can quantitatively detect the deoxy-Mb signal at ~10% deoxygenation in these calf experiments (Chung *et al.* 2005). Given the *in vitro* Mb P_{50} of 2.4 mmHg at 37 ˚C, the fact that the deoxy-Mb signal could not be detected in the resting state implies that the $P_{mb}O_2$ must saturate >90% of the Mb, or that $P_{mb}O_2$ is > 21.6 mmHg (Chung *et al.* 2005). Another study reported the Mb saturation level as 91 ± 1% in normoxia at rest (Richardson *et al.* 2006). In contrast, Schenkman *et al.* (2001) reported that the average baseline Mb saturation during perfusion with a $95\%O_2 + 5\%CO_2$ equilibrated buffer was 72% at rest. Thus, the resting value of $S_{mb}O_2$ remains controversial. However, under nitrogen-equilibrated buffer perfusion, the Δ[deoxy-Mb] signal no longer increases even following evoked muscle contraction. Mb is likely to be full deoxygenated under such conditions.

Conclusions

The present study has used NIRS to determine the intracellular O_2 dynamics and has observed that Mb desaturates progressively with an increase in oxygen demand, reflecting a progressive decrease in intracellular PO_2. The immediate decrease in $P_{mb}O_2$ leads to an expansion of the O_2 gradient, which enhances the O_2 flux to meet the increased $m\dot{V}O_2$. Moreover, the O_2 released from Mb likely supply the initial O_2 for respiration.

Acknowledgements

This research was supported by a Grant-in-Aid for Scientific Research from the Japanese Ministry of Education, Science, Sports and Culture (20680032, 21650167, KM), and partial support from the Yamaha Motor Foundation for Sports (KM) and the Nakatomi Foundation (KM).

References

Balaban RS, Bose S, French SA & Territo PR (2003). Role of calcium in metabolic signaling between cardiac sarcoplasmic reticulum and mitochondria *in vitro*. *Am J Physiol Cell Physiol* **284**, C285-C293.

Behnke BJ, Barstow TJ, Kindig CA, McDonough P, Musch TI & Poole DC (2002). Dynamics of oxygen uptake following exercise onset in rat skeletal muscle. *Respir Physiol Neurobiol* **133**, 229-239.

Behnke BJ, Kindig CA, Musch TI, Koga S & Poole DC (2001). Dynamics of microvascular oxygen pressure across the rest-exercise transition in rat skeletal muscle. *Respir Physiol* **126**, 53-63.

Box GEP, Hunter WG & Hunter JS (1978). Statistics for experimenters: An introduction to design, data analysis, and model building. New York: John Wiley & Sons.

Bylund-Fellenius AC, Walker PM, Elander A, Holm S, Holm J & Scherstén T (1981). Energy metabolism in relation to oxygen partial pressure in human skeletal muscle during exercise. *Biochem J* **200,** 247-255.

Chung YR, Molé PA, Sailasuta N, Tran TK, Hurd R & Jue T (2005). Control of respiration and bioenergetics during muscle contraction. *Am J Physiol Cell Physiol* **288**, C730-C738.

Gnaiger E, Steinlechner-Maran R, Méndez G, Eberl T & Margreiter R (1995). Control of mitochondrial and cellular respiration by oxygen. *J Bioenerg Biomembr* **27,** 583-596.

Hepple RT, Krause DJ, Hagen JL & Jackson CC (2003). $\dot{V}O_2$ max is unaffected by altering the temporal pattern of stimulation frequency in rat hindlimb *in situ*. *J Appl Physiol* 95, 705-711.

Honig CR, Gayeski TEJ & Groebe K (1997). Myoglobin and oxygen gradients. In *The Lung: Scientific Foundations*, pp. 1925-1933. Raven, Philadelphia.

Hogan MC (2001). Fall in intracellular PO_2 at the onset of contractions in Xenopus single skeletal muscle fibers. *J Appl Physiol* **90,** 1871-1876.

Jones DP (1986). Intracellular diffusion gradients of O_2 and ATP. *Am J Physiol Cell Physiol* **250**, C663-C675.

Jue T (2004). Bioenergetics implication of metabolic fluctuation during muscle contraction. In *Metabolomics by in vivo NMR*, ed. Shulman RG & Rothman DL, pp. 104-117. John Wiley, Chichester.

Kindig CA, Howlett RA & Hogan MC (2003). Effect of extracellular PO_2 on the fall in intracellular PO_2 in contracting single myocytes. *J Appl Physiol* **94**, 1964-1970.

Kreutzer U, Wang DS & Jue T (1992). Observing the ^{1}H NMR signal of the myoglobin Val-E11 in myocardium: an index of cellular oxygenation. *Proc Natl Acad Sci USA* **89**,

4731-4733.

Lin PC, Kreutzer U & Jue T (2007a). Anisotropy and temperature dependence of myoglobin translational diffusion in myocardium: implication for oxygen transport and cellular architecture. *Biophys J* **92**, 2608-2620.

Lin PC, Kreutzer U & Jue T (2007b). Myoglobin translational diffusion in rat myocardium and its implication on intracellular oxygen transport. *J Physiol* **578**, 595-603.

Masuda K, Takakura H, Furuichi Y, Iwase S & Jue T (2010). NIRS measurement of O_2 dynamics in contracting blood and buffer perfused hindlimb muscle. *Adv Exp Med Biol* **662**, 323-328.

Masuda K, Truscott K, Lin PC, Kreutzer U, Chung YR, Sriram R & Jue T (2008). Determination of myoglobin concentration in blood-perfused tissue. *Eur J Appl Physiol* **104**, 41-48.

McDonough P, Behnke BJ, Padilla DJ, Musch TI & Poole DC (2005). Control of microvascular oxygen pressures in rat muscles comprised of different fibre types. *J Physiol* **563**, 903-913.

Molé PA, Chung YR, Tran TK, Sailasuta N, Hurd R & Jue T (1999). Myoglobin desaturation with exercise intensity in human gastrocnemius muscle. *Am J Physiol Regul Integr Comp Physiol* **277**, R173-R180.

Papadopoulos S, Endeward V, Revesz-Walker B, Jurgens KD & Gros G (2001). Radial and longitudinal diffusion of myoglobin in single living heart and skeletal muscle cells. *Proc Natl Acad Sci USA* **98**, 5904-5909.

Philip LA & Dorothy SD (1971). *Respiration and Circulation*. Fed of Am Societies for Experimental Biology, Bethesda.

Poole DC, Ferreira LF, Behnke BJ, Barstow TJ & Jones AM (2007). The final frontier: oxygen flux into muscle at exercise onset. *Exerc Sport Sci Rev* **35**, 166-173.

Richardson RS, Duteil S, Wary C, Wray DW, Hoff J & Carlier PG (2006). Human skeletal muscle intracellular oxygenation: the impact of ambient oxygen availability. *J Physiol* **571**, 415-424.

Richardson RS, Noyszewski EA, Kendrick KF, Leigh JS & Wagner PD (1995). Myoglobin O_2 Desaturation During Exercise - Evidence of Limited O_2 Transport. *J Clin Invest* **96**, 1916-1926.

Rossiter HB, Ward SA, Doyle VL, Howe FA, Griffiths JR & Whipp BJ (1999). Inferences from pulmonary O_2 uptake with respect to intramuscular [phosphocreatine] kinetics during moderate exercise in humans. *J Physiol* **518**, 921-932.

Schenkman KA (2001). Cardiac performance as a function of intracellular oxygen tension in buffer-perfused hearts. *Am J Physiol Heart Circ Physiol* **281**, H2463-H2472.

Schenkman KA, Marble DR, Burns DH & Feigl EO (1997). Myoglobin oxygen dissociation by multiwavelength spectroscopy. *J Appl Physiol* **82**, 86-92.

Shiota M & Sugano T (1986). Characteristics of rat hindlimbs perfused with erythrocyte- and albumin-free medium. *Am J Physiol* **251,** C78-C84.

Takahashi E, Endoh H & Doi K (1999). Intracellular gradients of O_2 supply to mitochondria in actively respiring single cardiomyocyte of rats. *Am J Physiol* **276,** H718-H724.

Takahashi E, Endoh H & Doi K (2000). Visualization of myoglobin-facilitated mitochondrial O_2 delivery in a single isolated cardiomyocyte. *Biophys J* **78,** 3252-3259.

Takahashi E, Sato K, Endoh H, Xu ZL & Doi K (1998). Direct observation of radial intracellular PO_2 gradients in a single cardiomyocyte of the rat. *Am J Physiol* **275,** H225-H233.

Whipp BJ, Rossiter HB, Ward SA, Avery D, Doyle VL, Howe FA & Griffiths JR (1999). Simultaneous determination of muscle ^{31}P and O_2 uptake kinetics during whole body NMR spectroscopy. *J Appl Physiol* **86,** 742-747.

Wittenberg BA & Wittenberg JB (1989). Transport of oxygen in muscle. *Annu Rev Physiol* **51**, 857-878.

Figure Legends

Figure 1.

Representative muscle tension generation during muscle contraction for 120 sec from a single experiment.

Twitch muscle contractions were elicited every 1 sec (1 Hz). The target tension levels were set at 50%, 75% and 100%twitch tension under buffer-perfused condition, and were controlled by changing the voltage of the stimuli (3-8 volts). In this figure, a wave pattern of a single contraction and the time-course change of the twitch tension at the each exercise intensity were shown. No sign of fatigue was observed during muscle contraction regardless of the exercise intensity.

Figure 2.

Representative time course of the Δ[deoxy-Mb] and Δ[oxy-Mb] NIRS signals during different levels of twitch contractions (I-III) and under anoxic-perfusion (IV).

The arrows indicate the onset of contraction (I-III) and anoxic-perfusion (95%N_2 + 5%CO_2) (IV). Protocols I, II and III use 1 Hz stimulation to reach 50%, 75%, and 100% of maximal twitch tension The Δ[deoxy-Mb] and Δ[oxy-Mb] signals change immediately at the onset of contraction, and reach an Δ[deoxy-Mb] AP values of 4-15 μmol • cm (I-III). Under anoxia buffer perfusion condition, the Δ[deoxy-Mb] signal rises to higher AP value within 10 min.

Figure 3.

Representative kinetics of Mb saturation ($S_{mb}O_2$) and intracellular oxygen tension ($P_{mb}O_2$) during maximal twitch contraction (1 Hz).

The calculated $S_{mb}O_2$ (A) declines with an MRT of 44 sec. The $P_{mb}O_2$ (B), converted from the

$S_{mb}O_2$, using a P_{50} at 37 ˚C of 2.4 mmHg shows a faster and steeper decline than the $S_{mb}O_2$ curve (Schenkman *et al*. 1997). It has an MRT of 28 sec. At the maximal twitch tension, $S_{mb}O_2$ and $P_{mb}O_2$ reached 49% and 2.4 mmHg, respectively.

Figure 4.

Relationship between the Mb saturation ($S_{mb}O_2$) and work intensity during twitch contraction.

The $S_{mb}O_2$ during twitch contraction decreases linearly as a function of work intensity. The work intensity was normalized by maximal twitch tension in each animal. The regression line is based on mean values ($S_{mb}O_2$ = 93.95 - 0.45 • work intensity, r = - 0.81, $p < 0.01$, n = 6). Each data point represents the mean ± SD.

Figure 5.

Relationship between intracellular [O_2] and muscle oxygen consumption ($\Delta m\dot{V}O_2$) during twitch contraction.

Intracellular [O_2] (μM) decreased from 29.2 at rest to 8.5 ± 3.4, 5.0 ± 1.8 and 3.3 ± 1.0 at each tension level, and continues to gradually decrease as oxygen is consumed ($\Delta m\dot{V}O_2$) (Intracellular [O_2] = 29.2 -27.8 • (1-exp $^{(-0.08\ \Delta m\dot{V}O2)}$, r = 0.99). The $m\dot{V}O_2$ value represents the average value of $m\dot{V}O_2$ for 15 sec at the steady state during muscle contraction. The data point around the 30 μM of intracellular [O_2] represents intracellular [O_2] at rest of 29.2 μM. The curvilinear line is based on mean values (n = 6). Each data point represents the mean ± SD.

Figure 6.

Relationship between Mb O_2 release rate and muscle oxygen consumption ($\Delta m\dot{V}O_2$) at

the onset of contraction.

Mb released O_2 immediately after the onset of contraction, and the resulting oxygen release from Mb within myocyte increases with $\Delta m\dot{V}O_2$ (Mb O_2 release rate = 17.6 $\Delta m\dot{V}O_2$, $r = 0.71$, $p < 0.01$). The regression line is based on mean values. Each data point represents the mean ± SD.

Table 1

Physiological parameters at the each exercise intensity

Tension Level	50%	75%	100%
Muscle Tension (mN)	382.5 ± 61.7	567.0 ± 94.3 [a]	738.1 ± 122.9 [ab]
$\dot{m}VO_2$ at rest (μmol/g/min)	0.46 ± 0.11	0.47 ± 0.09	0.47 ± 0.11
$\dot{m}VO_2$ during contraction (μmol/g/min)	0.56 ± 0.10	0.63 ± 0.09	0.69 ± 0.12 [a]
$\Delta\dot{m}VO_2$ (μmol/g/min)	0.10 ± 0.04	0.16 ± 0.03	0.22 ± 0.07 [ab]
Rate increase in $\dot{m}VO_2$ (10^{-2} • μmol/g/min^2)	5.3 ± 1.8	7.8 ± 1.5	10.9 ± 3.4 [ab]
O_2 release rate of Mb (10^{-2} • μmol/g/min)	1.4 ± 0.5	2.8 ± 0.5 [a]	4.2 ± 0.7 [ab]

Values are mean ± SD (n = 6). $\Delta\dot{m}VO_2$ is net increase in $\dot{m}VO_2$ due to muscle contraction. Rate increase in $\dot{m}VO_2$ was calculated by dividing $\Delta\dot{m}VO_2$ by contraction time (2 min). The Mb O_2 release rate indicated the amount of [O_2] released from Mb per given time. All parameters except for resting $\dot{m}VO_2$ increased as increase in tension level. The superscripts indicate significant difference (a; vs. 50%, b; vs. 75%, $p < 0.05$).

Table 2

Lactate to pyruvate ratio at rest and at the each tension level

Rest	Tension Level		
	50%	75%	100%
19.8 ± 3.0	23.4 ± 3.4	22.8 ± 3.9	23.1 ± 4.3

Values are mean ± SD (n = 6) obtained after 2 min of muscle contraction. There was no significant difference in L/P during rest and contraction.

Table 3

$S_{mb}O_2$ and $P_{mb}O_2$ kinetics parameters during muscle contraction and anoxia buffer perfusion

Parameter (Unit)		Tension Level		
		50%	50%	50%
$S_{mb}O_2$ kinetics	Steady state value (%)	70.7 ± 7.1	59.2 ± 7.4 [a]	49.3 ± 7.3 [ab]
	AP (%)	-19.2 ± 7.1	-30.8 ± 7.4 [a]	-40.7 ± 7.3 [ab]
	MRT (sec)	63.7 ± 16.0	49.0 ± 7.9	44.6 ± 8.0 [a]
	$_{0.63}$AP/MRT (%/sec)	-0.19 ± 0.06	-0.40 ± 0.07 [a]	-0.58 ± 0.10 [ab]
$P_{mb}O_2$ kinetics	Steady state value (mmHg)	6.3 ± 2.5	3.7 ± 1.3 [a]	2.4 ± 0.7 [a]
	AP (mmHg)	-15.3 ± 2.5	-17.9 ± 1.3 [a]	-19.2 ± 0.8 [a]
	MRT (sec)	43.7 ± 4.2	34.5 ± 7.1 [a]	27.7 ± 3.1 [ab]
	$_{0.63}$AP/MRT (mmHg/sec)	-0.21 ± 0.03	-0.33 ± 0.06 [a]	-0.42 ± 0.04 [ab]

Values are mean ± SD (n = 6). The superscripts indicate significant difference (a; vs. 50%, b; vs. 75%, c; vs. 100%, $p < 0.05$).

Table 4

Estimation of $\dot{m}VO_2$ based on O_2 gradient between mean capillary PO_2 and intracellular PO_2 during rest and muscle contraction

Parameter (Unit)	Rest	Tension Level			Ref.
		50%	75%	100%	
$\dot{m}VO_2$ (μM/g/min)	465.7 ± 100.3	562.6 ± 96.7 [d]	626.2 ± 85.0 [d]	688.5 ± 120.1 [ad]	This paper
$\Delta\dot{m}VO_2$ (μM/g/min)	–	105.3 ± 36.2	156.0 ± 30.2	218.7 ± 67.2 [ab]	This paper
Microvascular PO_2 (mmHg)	31.4	(21.0)	(21.0)	21.0	Behnke *et al.* (2001)
Microvascular [O_2] (μM)	42.4	(28.4)	(28.4)	28.4	Behnke *et al.* (2001)
Intracellular PO_2 (mmHg)	21.6 ± 0.0	6.3 ± 2.5 [d]	3.7 ± 1.3 [ad]	2.4 ± 0.7 [ad]	This paper
Intracellular [O_2] (μM)	29.2 ± 0.0	8.5 ± 3.4 [d]	5.0 ± 1.8 [ad]	3.3 ± 1.0 [ad]	This paper
O_2 gradient (mmHg)	9.8 ± 0.0	14.7 ± 2.4 [d]	17.3 ± 1.3 [ad]	18.6 ± 0.7 [ad]	
O_2 gradient (μM)	13.2 ± 0.0	19.9 ± 3.4 [d]	23.4 ± 1.8 [ad]	25.0 ± 1.0 [ad]	
Estimated $\dot{m}VO_2$ (μM/g/min)	14.8 ± 0.7	89.0 ± 35.7 [d]	126.3 ± 22.5 [ad]	142.9 ± 14.8 [ad]	
Estimated $\Delta\dot{m}VO_2$ (μM/g/min)	–	74.2 ± 35.6	111.5 ± 21.9 [a]	128.1 ± 14.4 [a]	

Values are mean ± SD (n = 6). $\dot{m}VO_2$ and $\Delta\dot{m}VO_2$ was measured using O_2 electrodes. Both microvascular and intracellular [O_2] were calculated as values equilibrium with $P_{cap}O_2$ and $P_{mb}O_2$, respectively (microvascular or intracellular [O_2] = ($P_{cap}O_2$ or $P_{mb}O_2$) x O_2 solubility. The O_2 solubility is 0.00135 μmol/ml/mmHg at 37 ˚C (Philip and Dorothy, 1971)). The O_2 gradient represents the difference of [O_2] between microvasculature and myocyte. The estimated $\dot{m}VO_2$ was calculated by multiplying O_2 gradient and flow rate. $\Delta\dot{m}VO_2$ stands for net increase in $\dot{m}VO_2$ due to contraction. The superscripts indicate significant difference (a; vs. 50%, b; vs. 75%, c; vs. 100%, d; vs. Rest, $p < 0.05$).

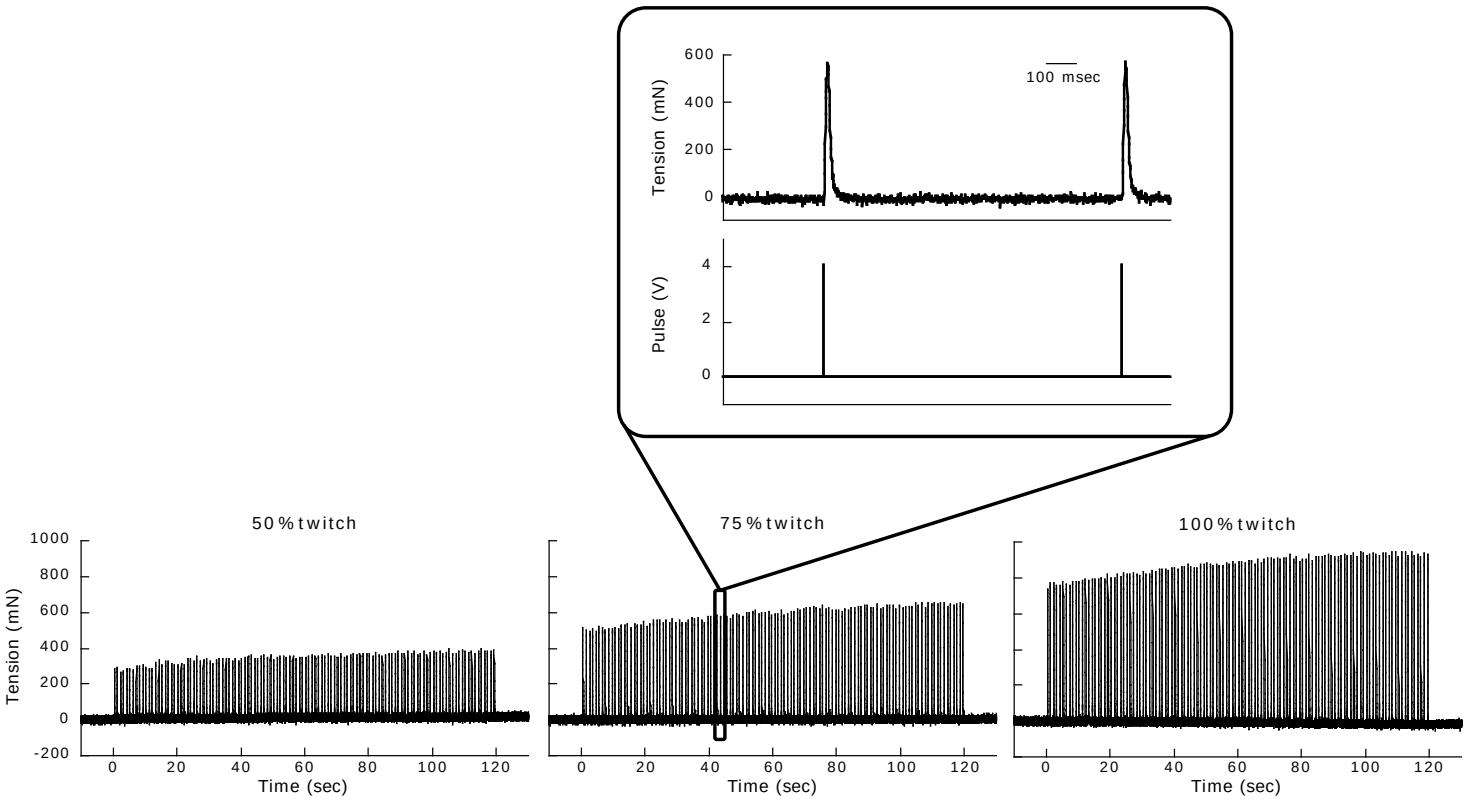
600
400
200
0
Tension (mN)
100 msec
4
2
0
Pulse (V)
50 % twitch
75 % twitch
100 % twitch
1000
800
600
400
200
0
-200
Tension (mN)
0
20
40
60
80
100
120
Time (sec)

Figure 1

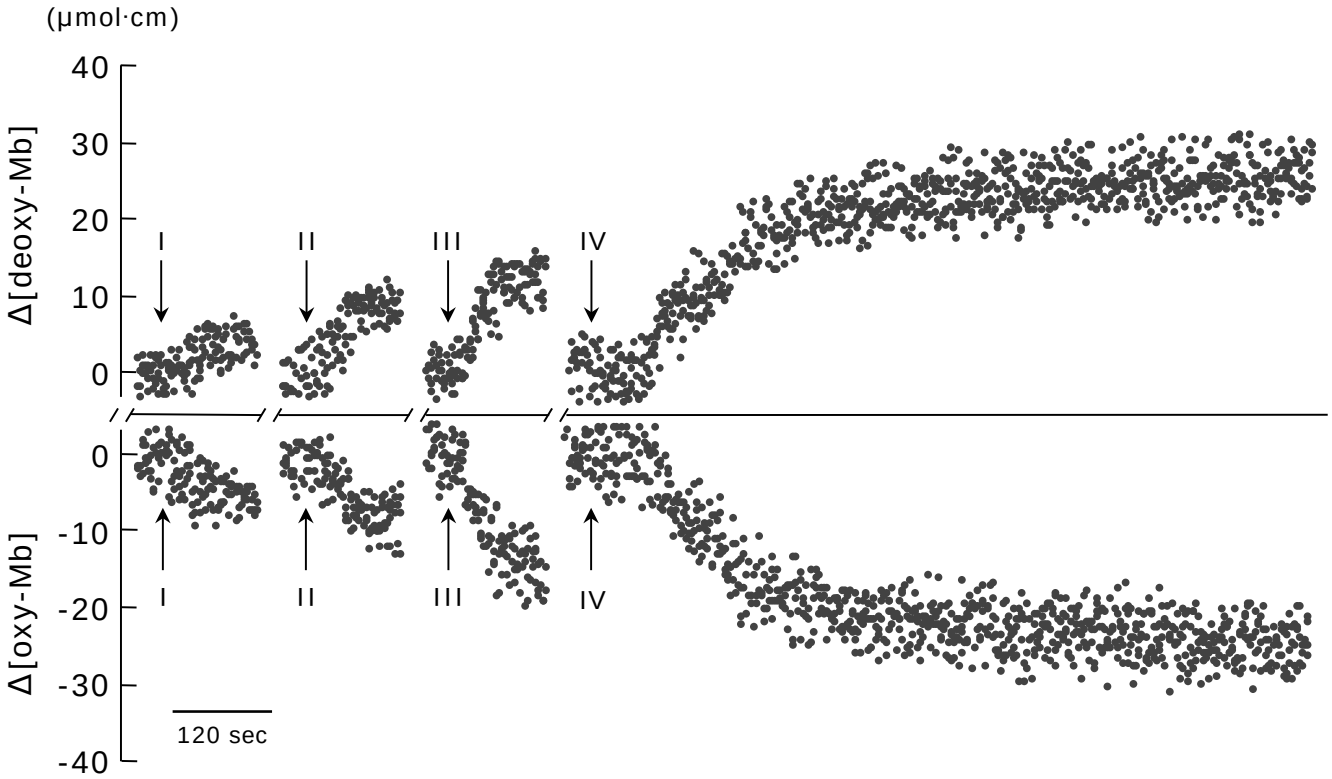
(µmol·cm)
40
30
20
10
0
Δ[deoxy-Mb]
I
II
III
IV
0
-10
-20
-30
-40
Δ[oxy-Mb]
I
II
III
IV
120 sec

Figure 2

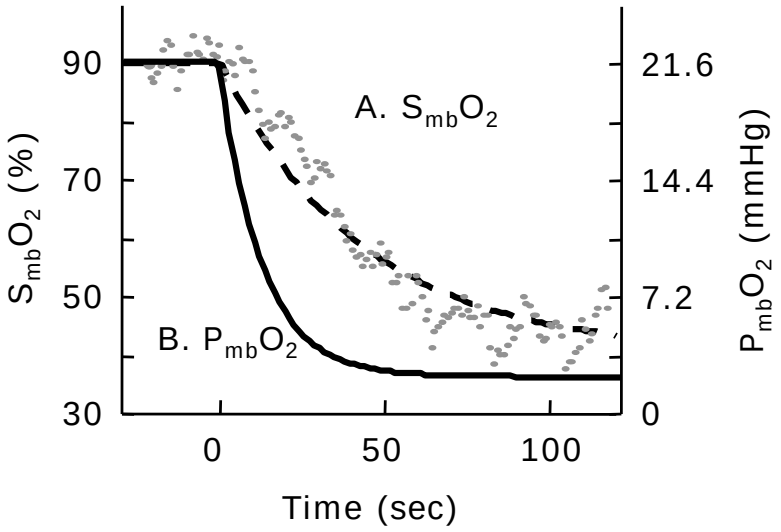
90
70
50
30
21.6
14.4
7.2
0
0
50
100
Time (sec)
A. $S_{mb}O_2$
B. $P_{mb}O_2$
$S_{mb}O_2$ (%)
$P_{mb}O_2$ (mmHg)

Figure 3

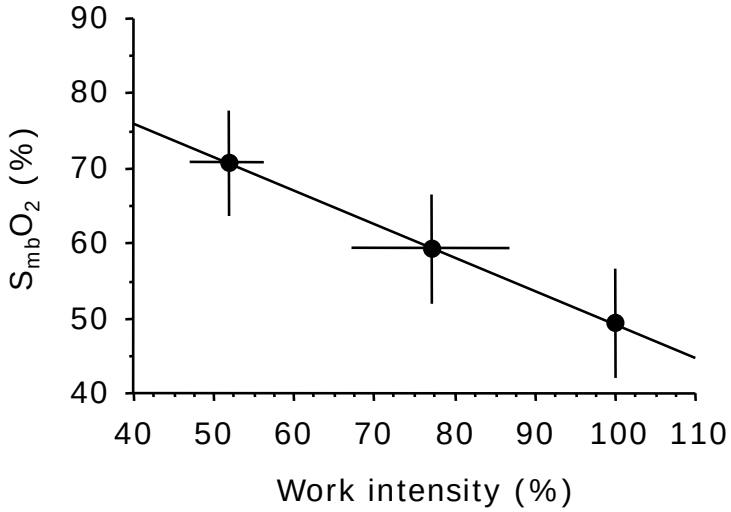

Figure 4

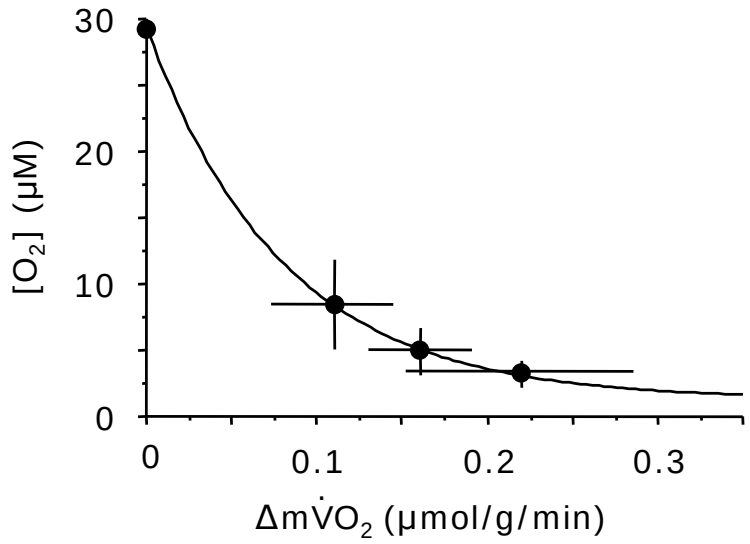

Figure 5

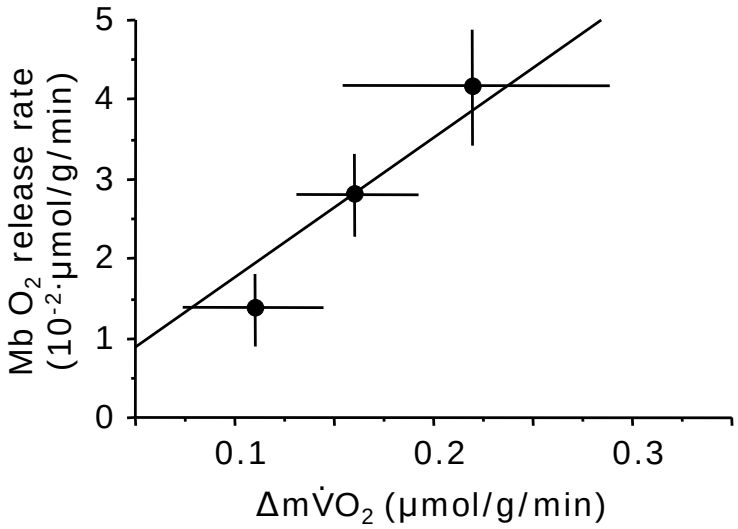
Mb O_2 release rate
(10^{-2}·µmol/g/min)
0
1
2
3
4
5
0.1
0.2
0.3
$\Delta m\dot{V}O_2$ (µmol/g/min)

Figure 6